33ND INTERNATIONAL COSMIC RAY CONFERENCE, RIO DE JANEIRO 2013
THE ASTROPARTICLE PHYSICS CONFERENCE

ICRC 2013

An Efficient Technique for the Reconstruction of Extensive Air Showers using Non-Imaging Cherenkov Measurements

DOUGLAS BERGMAN[1]

[1] *Dept. of Physics & Astronomy, University of Utah, Salt Lake City, Utah 84112 USA*

bergman@physics.utah.edu

Abstract: The reconstruction of air shower parameters such as energy and position of shower maximum, $X_{\max}$, implies that one knows on average how a shower with those parameters appears in the detector based on the detector response. This implies that one has a robust simulation of the detector response, but it also implies that there exists an accurate mapping between the fundamental shower parameters and the input to the detector simulation. Knowing the mapping between parameters and detector simulation one can perform an "Inverse Monte Carlo" simulation to fit the parameters to the observed data and thus reconstruct the energy and $X_{\max}$ of the initial air shower. In this poster, a technique is presented that maps the air shower parameters to the flux of Cherenkov photons at a given point on the ground and the time development of that flux. This is accomplished both by using full CORSIKA simulations and by employing a shower-universality model to generate Cherenkov light from an idealized shower. The results will show how well the efficient universality modeling compares to the computer-intensive CORSIKA simulations as well as the underlying potential of the non-imaging Cherenkov air shower measurement technique.

Keywords: Cosmic Rays, Extensive Air Shower Array, Non-imaging Air Cherenkov

The reconstruction of extensive air shower parameters from the data collected by arrays of non-imaging Cherenkov detectors traditionally relies on comparing data (total signal or signal width) from each counter to phenomenologically determined distributions. BLANCA[1] uses a fit to the Cherenkov Lateral Distribution (CLD) to determine the energy and depth of showers. Tunka[2] uses both the CLD and a fit to the lateral distribution of measurements of the Full Width Half-Max (FWHM) of the Cherenkov light pulse at each counter, denoted as the Cherenkov Width Lateral Distribution (CWLD), to determine the same shower parameters. While these techniques are sufficient in most cases to reconstruct shower parameters, a more robust reconstruction can be performed if one can predict the flux and time distribution of photons in each counter for a given set of shower parameters, specifically shower size and depth. The prediction should be free of any randomly generated variables so that one can fit the shower parameters by χ^2 minimization. This technique, called Inverse Monte Carlo (IMC) because the detector simulation routines will usually be identical to the ones used in the Monte Carlo simulation of the detector aperture and acceptance, is used by the HiRes[3] and Telescope Array[4] experiments when analyzing fluorescence data. The use of the IMC method when reconstructing non-imaging Cherenkov array data should allow the determination of the CLD and CWLD for the entire array.

While air shower variations limit the ability to predict the CLD and CWLD for the air shower resulting from a given primary cosmic ray, much of this variation can be attributed to variations of $X_{\max}$. The idea that showers with the same shower size and depth are identical is called Shower Universality. It has been developed in the context of ultra-high energy cosmic ray detectors using fluorescence detection techniques[5, 6, 7]. Shower Universality claims that knowing $N_{\max}$ and $X_{\max}$ is sufficient to predict the electron energy distribution, the electron angular distribution, the electron lateral distribution and the electron time delay distribution *at every point in the shower*. It does this using parameterizations of the distributions which depend only on the position within the shower with respect to $X_{\max}$ and the parameters of the atmosphere at that point in the shower. This paper shows how Shower Universality, which involves the electromagnetic component of the shower, may be extended to include the Cherenkov radiation component and thus be useful for non-imaging Cherenkov array data reconstruction.

1 Mathematical Treatment

The angular distribution of Cherenkov photons, g_γ produced at a given point in the shower is the convolution of the electron angular distribution, g_e, with the Cherenkov cone produced by each electron. We will, however, derive g_γ through direct integration of the fraction electrons going into an element of solid angle $\mathrm{d}\Omega_e$ which then give rise to a Cherenkov photon going into another element of solid angle $\mathrm{d}\Omega_\gamma$. We fix $\mathrm{d}\Omega_\gamma$ to correspond to an actual counter in the array.

The geometric variables used in the calculation are defined in Figure 1. $\hat{\mathbf{n}}$ is the direction of the shower (core), $\hat{\mathbf{e}}$ is the direction taken by the electron, and $\hat{\gamma}$ is the direction taken by the photon. For a given counter $\hat{\gamma}$ is fixed with respect to $\hat{\mathbf{n}}$. θ_e is the angle between $\hat{\mathbf{n}}$ and $\hat{\mathbf{e}}$, θ_γ is the angle between $\hat{\mathbf{e}}$ and $\hat{\gamma}$ and θ is the fixed angle between $\hat{\mathbf{n}}$ and $\hat{\gamma}$. Spherical trigonometry applies, and the interior angles of the spherical triangle are labeled ϕ with the subscript from the opposite leg. The Law Of Cosines, $\cos\theta_e = \cos\theta\cos\theta_\gamma - \sin\theta\sin\theta_\gamma\cos\phi_e$ allows one to calculate θ_e from the other two legs and their opening angle. We will thus consider θ_e to be a function of θ_γ and ϕ_e with θ being fixed.

The electron energy distribution at a given point in a shower is typically designated $f_e(E_e;s) = \frac{\mathrm{d}N_e}{\mathrm{d}l}$ where

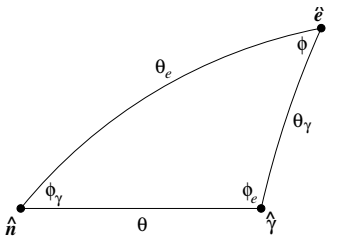

Fig. 1: The angles involved in producing a Cherenkov photon at an angle θ from the shower axis. The interior (ϕ) angles are labeled after the opposite side (θ).

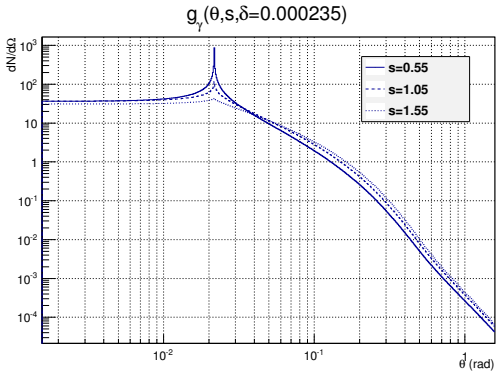

Fig. 2: Three examples of g_γ at a specific atmospheric height (where $\delta = 0.000235$). The angular distribution for showers of age $s = 0.55$, 1.05 and 1.55 are shown.

$l = \ln E_e$. (We will consistently use l to denote the logarithm of energy, $l = \ln E$.) f_e has been parameterized by several groups[6, 7]. The electron angular distribution, g_e, is determined for electrons of a given *energy*, $g_e(\theta_e; E_e) = \frac{dN_e}{d\Omega_e}$. Cylindrical symmetry is assumed. Combining f_e and g_e, we find that the fraction of electrons at a given depth in the shower with a given energy and a going in the direction $\hat{\mathbf{e}}$ is

$$dN_e = f_e(E_e; s)\, g_e(\theta_e; E_e)\, dl\, d\Omega_e$$

The electrons going in toward $\hat{\mathbf{e}}$ will produce Cherenkov photons according to their energy and path length. If we divide out the maximum photon yield $dN_\gamma/dX(E_e \gg E_{\rm Th})$, where $E_{\rm Th}$ is the Cherenkov threshold, we're left with a relative photon yield of $Y_{\check{\rm C}} = 1 - (E_e/E_{\rm Th})^2$. Some of these photons will go into the solid angle about $\hat{\gamma}$ as long as $\theta_\gamma = \theta_{\check{\rm C}}$. Thus the fraction of photons going towards $\hat{\gamma}$ from electrons going towards $\hat{\mathbf{e}}$ is

$$dN_\gamma = Y_{\check{\rm C}}\, \delta(\theta_\gamma - \theta_{\check{\rm C}})\, \frac{d\Omega_\gamma}{2\pi}$$

The key to easily performing the integral is to realize that $d\Omega_e$ can be defined in terms of variables related to $\hat{\gamma}$ rather than with respect to $\hat{\mathbf{n}}$ as described above. Thus, $d\Omega_e = \sin\theta_\gamma\, d\phi_e\, d\theta_\gamma$. Likewise $d\Omega_\gamma = \sin\theta\, d\phi_{\hat{\mathbf{n}},\hat{\gamma}}\, d\theta$, where $\phi_{\hat{\mathbf{n}},\hat{\gamma}}$ is the arbitrary azimuthal angle between $\hat{\mathbf{n}}$ and $\hat{\gamma}$. Thus the fraction of all Cherenkov photons produced at a point in the shower going into $\hat{\gamma}$ is $g_\gamma(\theta; s, \delta)\, d\Omega_\gamma$,

$$\begin{aligned} g_\gamma &= \int d\Omega_e \int_{l_{\rm Th}}^{\infty} dl\; Y_{\check{\rm C}}\, f_e\, g_e\, \delta(\theta_\gamma - \theta_{\check{\rm C}}) \\ &= \int_0^{1/n} d\theta_\gamma \sin\theta_\gamma Y_{\check{\rm C}}(l_\gamma)\, f_e(l_\gamma) \int_0^{2\pi} d\phi_e\, \frac{g_e(\theta_e; l_\gamma)}{\left|\theta'_{\check{\rm C}}(l_\gamma)\right|} \end{aligned}$$

where the θ dependence is implicit in $l_{\rm Th}$, $l_\gamma = l(\theta_\gamma)$ (i.e. the energy at which the Cherenkov angle is θ_γ), and

$$\theta'_{\check{\rm C}}(l_\gamma) = \left.\frac{d\theta_{\check{\rm C}}}{dl}\right|_{l_\gamma}.$$

Switching from $d\theta_\gamma$ to l_γ as an integration variable makes for more robust numerical integration, and is especially simple because $\left|\theta'_{\check{\rm C}}(l_\gamma)\right|$ is just the Jacobian for this transformation. In this case $\theta_\gamma = \theta_\gamma(l)$. Thus we have

$$g_\gamma = \int_{l_{\rm Th}}^{\infty} dl_\gamma \sin\theta_\gamma Y_{\check{\rm C}}(l_\gamma)\, f_e(l_\gamma) \int_0^{2\pi} g_e(\theta_e; l_\gamma)\, d\phi_e \qquad (1)$$

In practice the upper limit of the outer integral is determined by the range of the parameterization of g_e.

The integrands above were implemented as C++ functions in ROOT, and the ROOT built-in integrations routines were used to perform the numeric integration. With a lax setting on the precision of the two integrations (10^{-5} on the inner integral, 10^{-4} on the outer) the time for the total integration at a few hundred θ values for a given s and δ was reduced to a few seconds. An example output of the calculation is shown in Figure 2. Note that the function has been explicitly normalized after the calculation. Also, θ values have been selected at logarithmic points along the axis. This result also uses the parameterization of the electron angular distribution g_e developed in the next section.

The g_γ values may be tabulated into a lookup table for later use. One must take care to select the points carefully to retain the most salient feature, the sharp peak visible in Figure 2 at low values of s. Logarithmic sampling in θ is necessary, with enough points in θ to capture the shape of the peak. The points in δ must be close enough that the peak does not move by more than one bin in θ between successive samples in δ. Sampling in s is less demanding as the peak does not move as s changes. With these safeguards, the value of g_γ may be safely interpolated from the stored values in the lookup table.

2 Electron Angular Distribution

The election angular distribution has been parameterized by a number of different groups[5, 7]. However, these studies have been done for use in UHECR fluorescence experiments where electron energies are only considered up to the GeV scale and electron angles only down to the degree scale. For use in Cherenkov detectors, a parameterization of g_e should extend in energy up to the TeV scale and down in angle to well below the Cherenkov cone angle at any point of the shower.

We have chosen to extend the parameterization of Giller *et al*[5], with an exponential distribution for the bulk of the shower and a power law distribution for the tail. However, rather than joining the two functional forms at some angle, we have taken the sum of two distributions. Our parameterization is thus

$$g_e(\theta) = a_1 e^{-c_1\theta - c_2\theta^2} + a_2(1 + \theta/\theta_0)^{-r}$$

where a_1, c_1, c_2, a_2, θ_0 and r are implicitly functions of E.

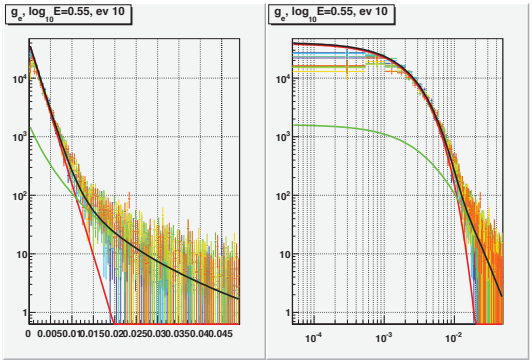

Fig. 3: A parameterized fit to the electron angular distribution at $10^{0.55}$ GeV is shown in black. The two components of the fit are shown in red (exponential) and green (power law). The electron distribution from 10 Corsika events are shown as variously colored data points.

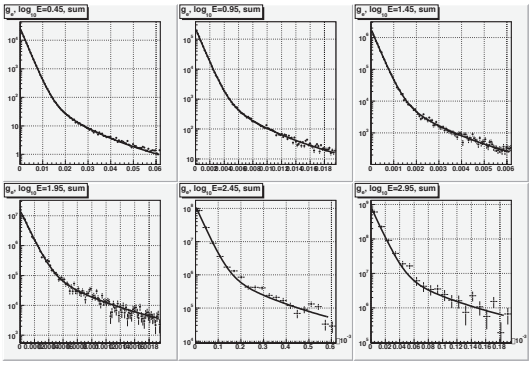

Fig. 4: Comparison of the parameterization presented in this paper with the average of 10 Corsika showers at a primary cosmic ray energy of 3.16 PeV. Comparisons shown at electron energies of $10^{0.44}$, $10^{0.95}$, $10^{1.45}$, $10^{1.95}$, $10^{2.45}$ and $10^{2.95}$ GeV.

The parameters were chosen by averaging the electron distributions from 30 Corsika-generated showers, evenly split between proton and iron primaries and between energies of 3.16, 10 and 31.6 PeV energies. The result of the parameterization is shown in Figure 3 for electrons of energy 3.55 GeV. Also shown in the figure are the 10 events with a primary energy of 3.16 PeV. The large variation between individual events in the simulated values for g_e indicate that universality holds better for the exponential portion of the distribution than for the power law part.

We assumed pure power laws for the scale parameters c_1 and c_2 and nearly pure for θ_0 and let the normalization parameters adjust in the fit. We find

$$
\begin{aligned}
a_1(E) &= a_{10}E^{a_{11}+a_{12}l+a_{13}l^2} \\
c_1(E) &= c_{10}E^{c_{11}} \\
c_2(E) &= c_{20}E^{c_{21}} \\
a_2(E) &= \begin{cases} a_{20}E^{a_{21}}+a_{22} & E \geq E_b \\ \frac{a_{20}E_b^{a_{21}}+a_{22}-a_{24}}{E_b^{a_{23}}}\left(E^{a_{23}}+a_{24}\right) & E < E_b \end{cases} \\
\theta_0(E) &= \begin{cases} p_0E^{p_1} & E \geq E_c \\ p_0E_c^{p_1-p_2}E^{p_2} & E < E_c \end{cases} \\
r(E) &= \begin{cases} r_0 & E \geq E_d \\ r_1E^{r_2+r_3l} & E < E_d \end{cases}
\end{aligned}
$$

where $E_b = 10^{-1.5}$ GeV, $E_c = 10^{-1.4}$ GeV, $E_d = 10^{r_2/r_3}$ GeV and $l = \log E$. The lower level parameters are

i	0	1	2	3	4
a_{1i}	359000	1.82	0.0366	0.0138	
c_{1i}	163	0.952			
c_{2i}	183	0.921			
a_{2i}	340	1.74	6.04	4.29	2.51
p_i	0.0204	-0.790	-2.20		
r_i	3.70	0.132	-0.134	0.538	

Comparison of this parameterization with the average Corsika showers in shown in Figure 4.

3 Results and Comparisons

To check the quality of the model of Cherenkov light production given by Equation 1, we have simulated the arrival time distributions for Cherenkov light at counters various distances from the shower core. The shower was broken into longitudinal sections which correspond to the time binning specified for the given counter. This avoids sampling issues and gives very smooth signal time distributions. The steps were sometimes further subdivided if shower parameters changed significantly within a step. In each step we multiply the calculated g_γ by the step size dX and the solid angle subtended by the counter from that step dΩ. We also multiply by the maximum Cherenkov yield (the relative part being taken into account in the integration) and the shower size as given by a Gaisser-Hillas parameterization. When comparing the universality model results against Corsika predictions, we used the Corsika Gaisser-Hillas fit parameters as inputs to the model predictions.

Comparisons with a specific Corsika generated shower are shown in Figure 5. The shower was a proton initiated shower with a primary energy of $10^{15.5}$ eV. The Gaisser-Hillas parameters of the shower are $N_{\max} = 1.8 \times 10^6$, $X_{\max} = 575$ g/cm^2, $x_0 = -35$ g/cm^2 and $\Lambda = 84$ g/cm^2. No atmospheric photon absorption was applied in either the universality model or in the Corsika calculation.

It is clear that the shower-as-line assumption used in the universality model doesn't work for as well for counters close to the shower core, where the spread of the shower is of the same order as the counter distance. It appears that longitudinal distribution of shower electrons makes the time distribution sharper for counters within about 120 m. However, even for these counters, the universality model predicts the shape of the tail fairly well. At distances well beyond 120 m, the model predicts the shape quite well.

Figure 6 shows a comparison of the CWLD over the full range of counters. The variability in the widths comes from the statistical variation within the Corsika simulation. Figure 7 shows the CWLD for vertical showers with $X_{\max}$ from 400–900 g/cm^2.

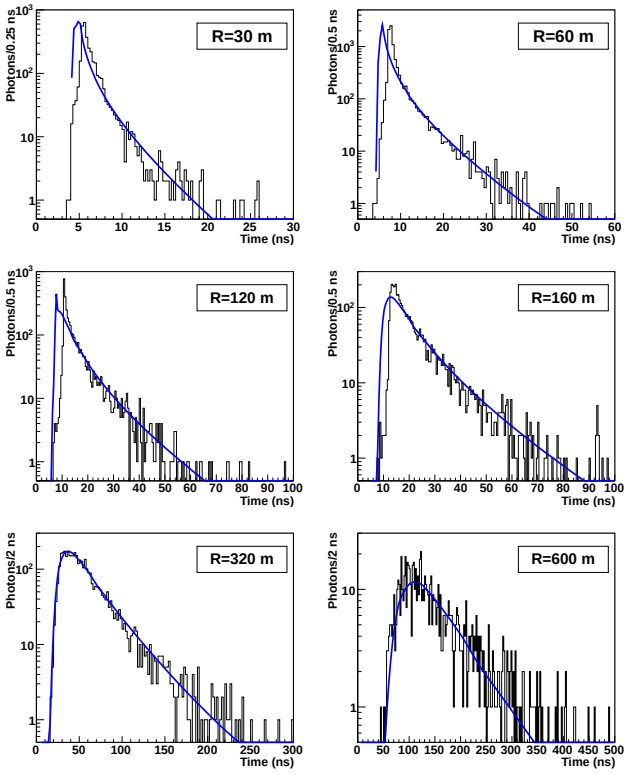

Fig. 5: Arrival time distributions for counters at 30, 60, 120, 160 320, and 600 m from the shower core. The universality model is shown in blue, while the Corsika calculation is shown in black. The 120-m universality simulation shows the narrow and broad contributions to the FWHM at parity. The narrow contribution dominates at smaller distances while the broad contribution dominates at larger.

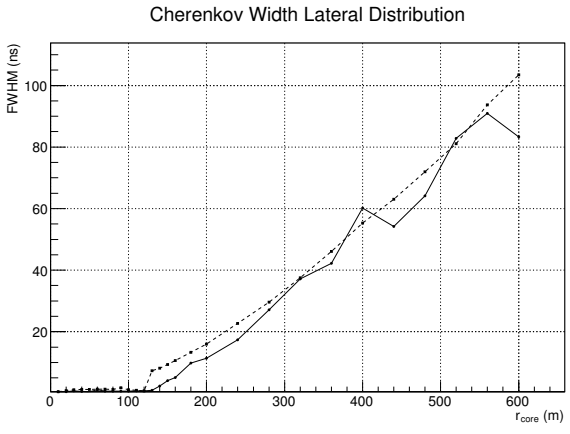

Fig. 6: Comparison of the Cherenkov Width Lateral Distribution between Corsika simulation (sold line, circle) and the universality model (dashed line, square). The shower being compared had Gaisser-Hillas parameters $N_{\max} = 1.8 \times 10^6$, $X_{\max} = 575$ g/cm^2, $x_0 = -35$ g/cm^2 and $\Lambda = 84$ g/cm^2. The full-width half max of the Cherenkov photon arrival time distribution at the ground is shown for each model versus the distance along the ground from the shower core. The Corsika simulation arrival time distributions are rebinned to allow reliable measurements of the FWHM.

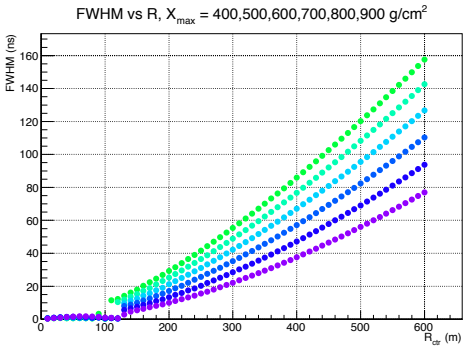

Fig. 7: The CWLD for vertical showers with $X_{\max}$ from 400–900 g/cm^2. The discontinuities at around 120 m come from the change in the dominant FWHM component.

4 Discussion

The use of shower universality to model the response of non-imaging Cherenkov counters shows promise, but must be developed further to gain usefulness. The simplest use of the model, with a linear shower and only electron energies and angles taken into account, is in qualitative agreement with detailed shower simulations. It reproduces both the CLD and CWLD at distances from the core greater than about 30 m, though the transition from core-dominated (narrow) to bulk-dominated (wide) widths at about 120 m is much sharper in the universality model than in the shower simulations.

Two obvious improvements to the universality model present themselves. The first is to include the time-delay of the electrons within the shower. The time delay of the electrons has been parameterized as a function of energy by Lafebre *et al*[7]. The second improvement is to model the lateral distribution of the electrons using the NKG distribution[10, 11]. Implementation of the NKG sampling is difficult to do with sufficient sampling to retain the smooth curves currently in place or without increasing the simulation time drastically.

This work supported by the National Science Foundation grant PHY-1069280. Special thanks to Gordon Thomson and John Krizmanic for useful discussions.

References

[1] J. Fowler, et al., Astropart. Phys. 15 (2001) 49.
[2] V. V. Prosin, et al., Nucl. Phys. B Proc. Supl. 190 (247).
[3] R. U. Abbasi, et al., Phys. Rev. Lett. 100 (2008) 101101.
[4] D. R. Bergman, et al., Proceedings of the 32nd ICRC (Beijing), Vol. 2, 2011, pp. 265.
[5] M. Giller, et al., J. Phys. **G** 30 (2004) 97.
[6] F. Nerling, et al., Astropart. Phys. 24 (2006) 421.
[7] S. Lafebre, et al., Astropart. Phys. 31 (2009) 243.
[8] M. Giller, G. Wieczorek, Astropart. Phys. 31 (2009) 212.
[9] J. R. Patterson, A. M. Hillas, J. Phys. **G** 9 (1983) 323.
[10] K. Kamata, J. Nishimura, Prog. Theor. Phys. Suppl. 6 (1958) 93.
[11] K. Greisen, Progres in Cosmic Ray Physics, Vol. 3, North Holland, 1956, Ch. 1.